Determination of Total Hip Replacement stem insertion endpoint and stability assessment by vibration analysis: first experiences with per-operative measurements

Leonard C. Pastrav [*], Siegfried V. N. Jaecques [*], Michiel Mulier [**], Georges Van der Perre [*]
[*] Katholieke Universiteit Leuven, Division of Biomechanics and Engineering Design (BMGO), Leuven, Belgium
[**] University Hospital Leuven, Department of Orthopaedic Surgery, Leuven, Belgium
email: **cezar.pastrav@mech.kuleuven.be**

Abstract

The assessment of the primary stability of cementless implants still remains a subjective factor in total hip replacement (THR) and, as a consequence, the excessive press-fitting of a THR component can be the cause of intra-operative fractures. Objective information about the stability of implant-bone structures can be obtained using methods based on vibration analysis. After extensive *in vitro* studies, a per-operative protocol was designed to detect the insertion endpoint and/or to assess the stability of custom made hip prostheses. The experiments were performed on cementless hip stems and on hybrid hip stems that were partially cemented distally. This paper presents the frequency response function evolution during the hip stem insertion in the femur, in per-operative conditions.

1 Introduction

The initial stability seems to be very important for any prosthetic implant, but the objective assessment of this parameter for cementless hip stems remains a challenge. Surgeons rely mainly on experience to evaluate the extent of stem stability and the insertion end point. Excessive press-fitting of a total hip replacement component (Figure 1) can cause intra-operative fractures with an incidence of up to 30% in revision cases [1].

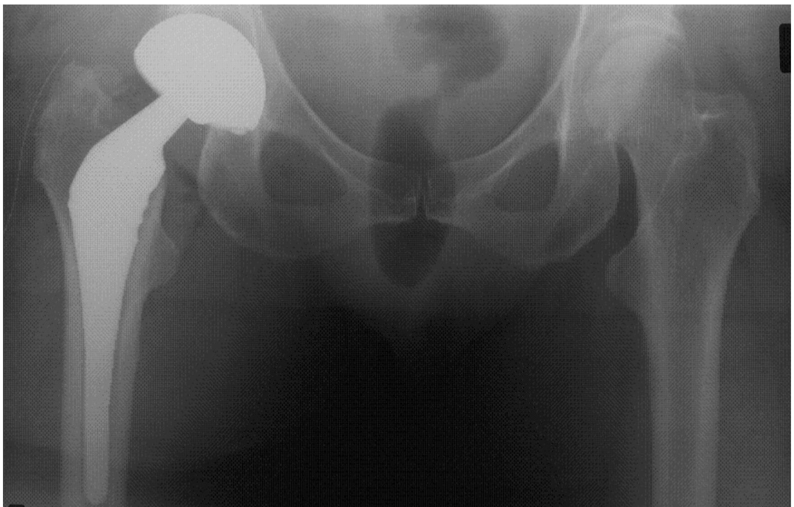

Figure 1: Total Hip Replacement (THR)

In 1932 Lippmann used auscultatory percussion for the examination of clavicle fractures [2]. Since then, more sophisticated methods based on vibration analysis have been successfully used to determine bone mechanical properties *in vitro* as well as *in vivo* [3, 4, 5, 6, 7], to monitor fracture healing [8, 9, 10], to quantify the fixation of dental implants [11, 12, 13], and to assess the mechanical properties of the hip stem/femur structure. A limited number of studies prove the feasibility of detecting several forms of loosening with vibration analysis, *in vitro* and in *vivo* [14, 15, 16, 17, 18, 19].

In a previous study [20], it was confirmed that the imperfections in the connection between a THR prosthetic stem and a femur can most sensitively be detected by observing shifts in the resonance frequency of the higher vibration modes of the femur/prosthesis system. This observation is in accordance with the work of Qi et al who state that the most sensitive frequency band for observing defects in the femur/prosthesis connection is above 2500 Hz [21]. An experimental study [22] performed on artificial human femora (Sawbone® nr. 3306, Left Large Composite Femur, **www.sawbones.com**) has shown that the evolution of the frequency response function (FRF) can be used to detect the insertion end point as well.

This paper presents the per-operative protocol derived from the previous *in vitro* studies and the first results obtained in a pilot experimental study performed in per-operative conditions.

2 Materials and methods

The per-operative protocol was mainly designed to detect the insertion endpoint and to assess the stability of cementless custom made hip prostheses (Advanced Custom Made Implants, Leuven, Belgium). The surgeon inserts the implant in the femoral canal through hammer blows. After each blow, the FRF of the implant-bone structure is measured directly on the prosthesis neck in the range 0-12.5 kHz. The FRF change indicates the evolution of the stiffness of the implant-bone structure and, as a consequence, the evolution of the implant stability. The hammering is stopped when the FRF graph does not change noticeably anymore. Extra blows will not improve the prosthesis stability but will increase the fracture risk.

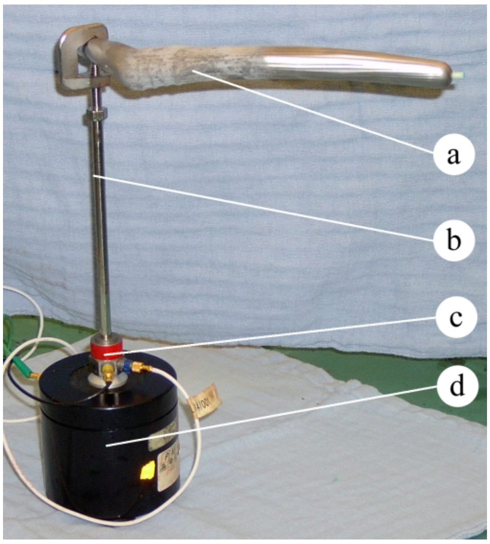

Figure 2: Experimental setup

a. hip stem
b. stinger and clamping system
c. impedance head
d. shaker

The prosthesis neck is attached to a shaker (Bruel & Kjaer model 4810) using a stinger provided with a clamping system. The excitation is realized through white noise in the range 0-12.5 kHz. In an earlier version, the input force was measured with a force cell mounted between the shaker and the stinger. The response acceleration was measured using an accelerometer attached to the prosthesis neck with orthopaedic wax.

However, during a test on a cadaver, it was observed that is very difficult to maintain a correct position of the accelerometer on the prosthesis neck and, in order to reduce the subjective factors, the accelerometer and the force cell were replaced by an impedance head (PCB Piezotronics model nr 288D01) which measures the input force and the response acceleration in the same point. The final setup is shown in Figure 2.

The FRF was measured and recorded by a Pimento vibration analyser (LMS International) connected to a portable computer provided with the appropriate software (Pimento 5.2, LMS International). The vibration analyser generates the excitation signal which is amplified and sent to the shaker. The vibration analyser, the portable computer and the amplifier were installed in the surgical theatre but outside the so-called laminar flow area (Figure 3).

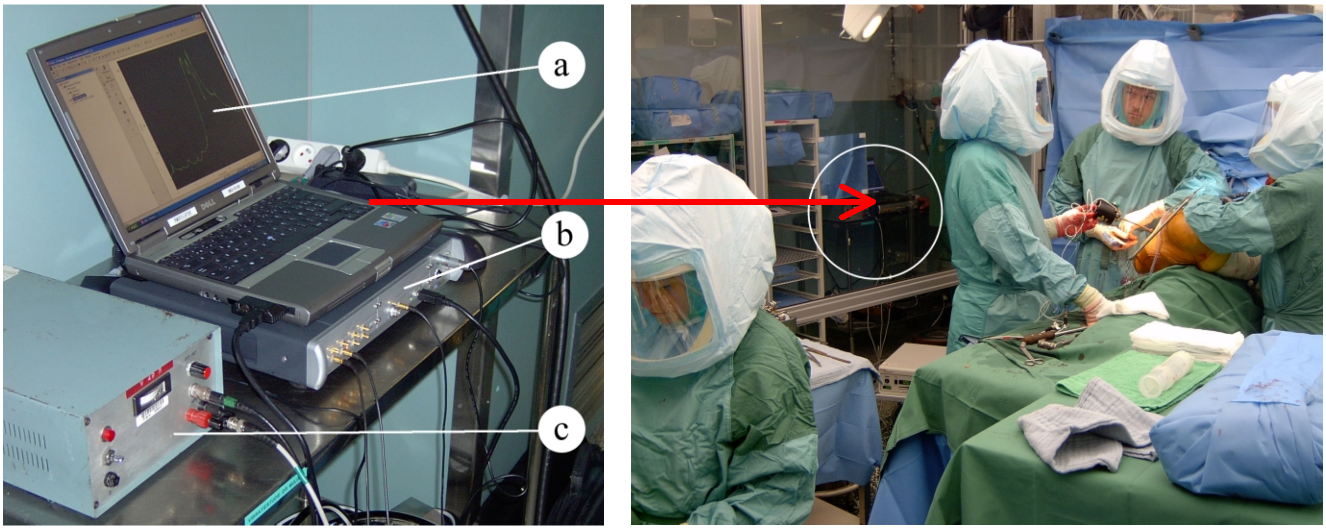

Figure 3: Measuring hardware (left) and surgical theatre (right)

a. portable computer
b. vibration analyser Pimento
c. power amplifier

The per-operative protocol presented above was adapted to assess the stability of custom made hybrid hip stems (Advanced Custom Made Implants, Leuven, Belgium) that were partially cemented distally.

In a first stage, the surgeon inserts the stem completely in the femur without cement, for a trial reduction of the artificial joint. In a later stage, the stem is removed, cement is introduced in the distal part of the femoral canal, the stem is re-introduced and after the cement has fully cured, the implant is supposed to be well fixed. The FRF is measured in both stages using the same method as in the cementless stems case (Figure 4).

Volunteer patients were included in this study after informed consent and approval by the institutional review board.

To analyse the differences between the FRF graphs, the Pearson's product moment correlation coefficient and the normalised cross correlation function were used.

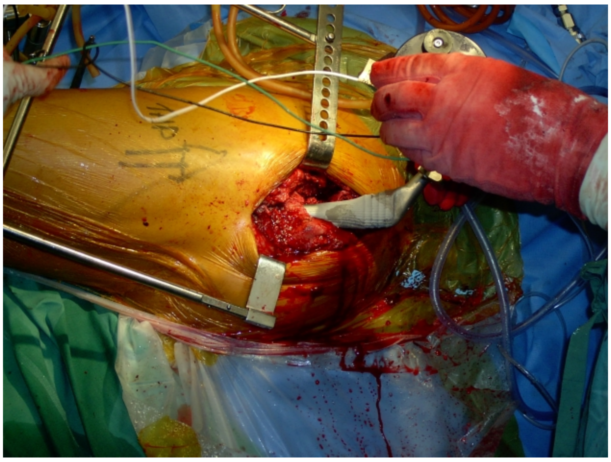

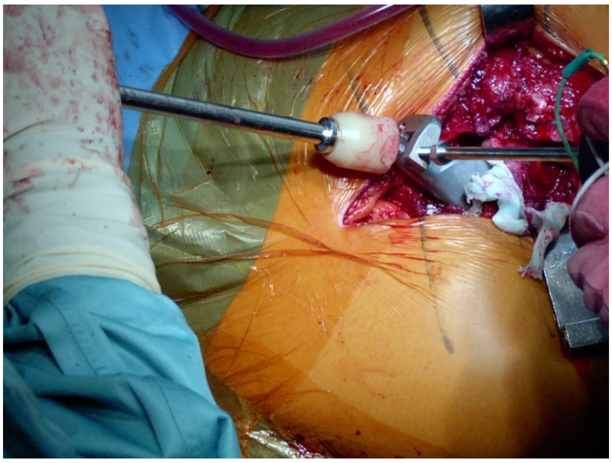

Figure 4: Hip stem insertion

Left: cementless; **Right:** partially cemented

3 Results

3.1 Partially cemented stems

Nine cases of partially cemented prostheses were studied. In seven cases (77.8%) an important difference was observed between the FRF graph corresponding to the cementless stage and the FRF graph corresponding to the cemented stage, in frequency and amplitude. Two typical examples are shown in fig. 5 and 6.

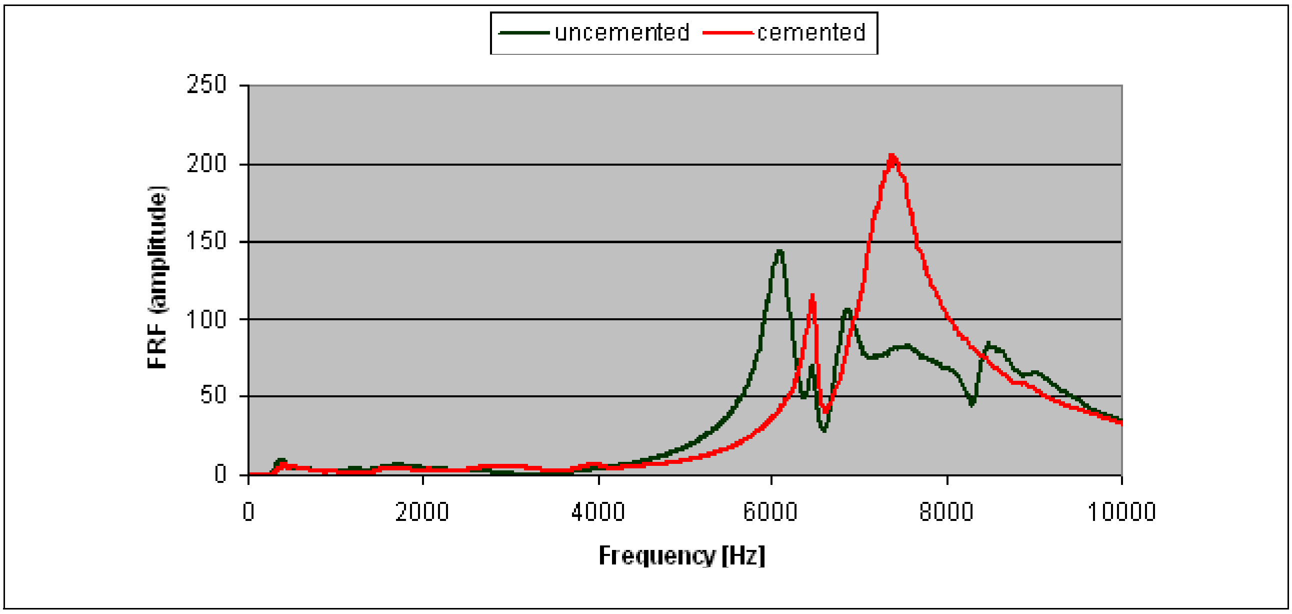

Figure 5: Partially cemented stem completely inserted in the femur (example case 1)
FRF graphs for two stages: without cement (black) and cemented (red)

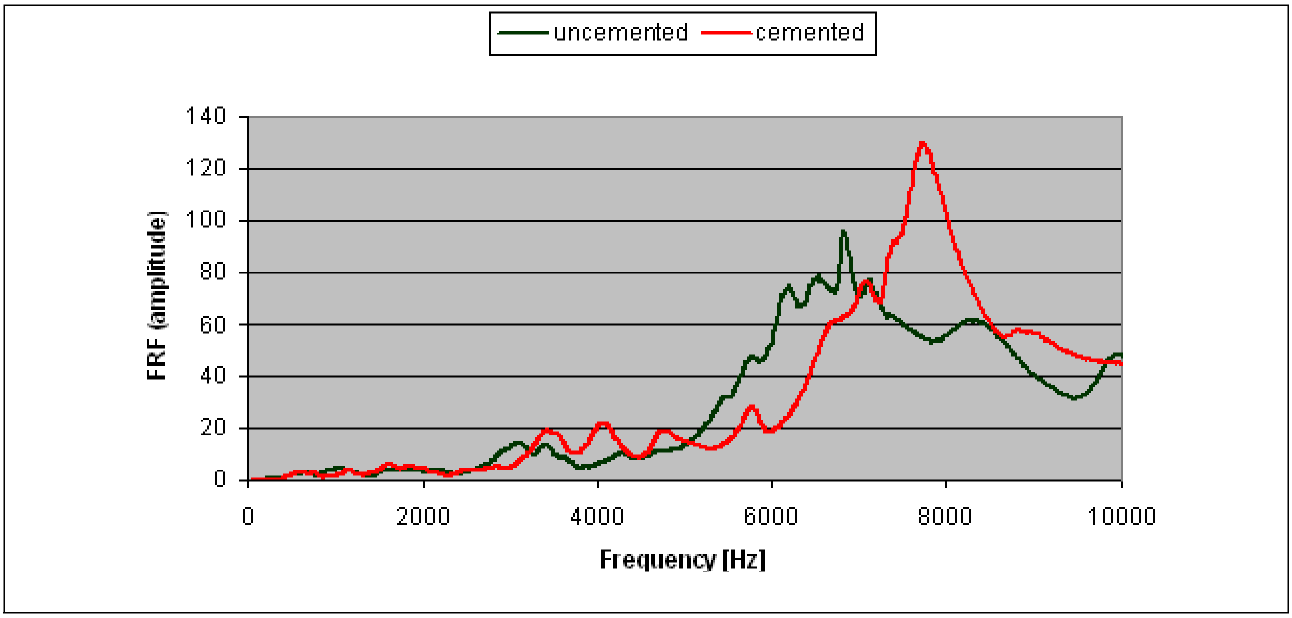

Figure 6: Partially cemented stem completely inserted in the femur (example case 2)
FRF graphs for two stages: without cement (black) and cemented (red)

In the other two cases, although an amplitude alteration could be noticed, the resonance frequencies did not substantially change. Fig. 7 shows one of those two cases.

For all nine cases, the FRF was measured in the second stage after the hardening process of the cement had ended.

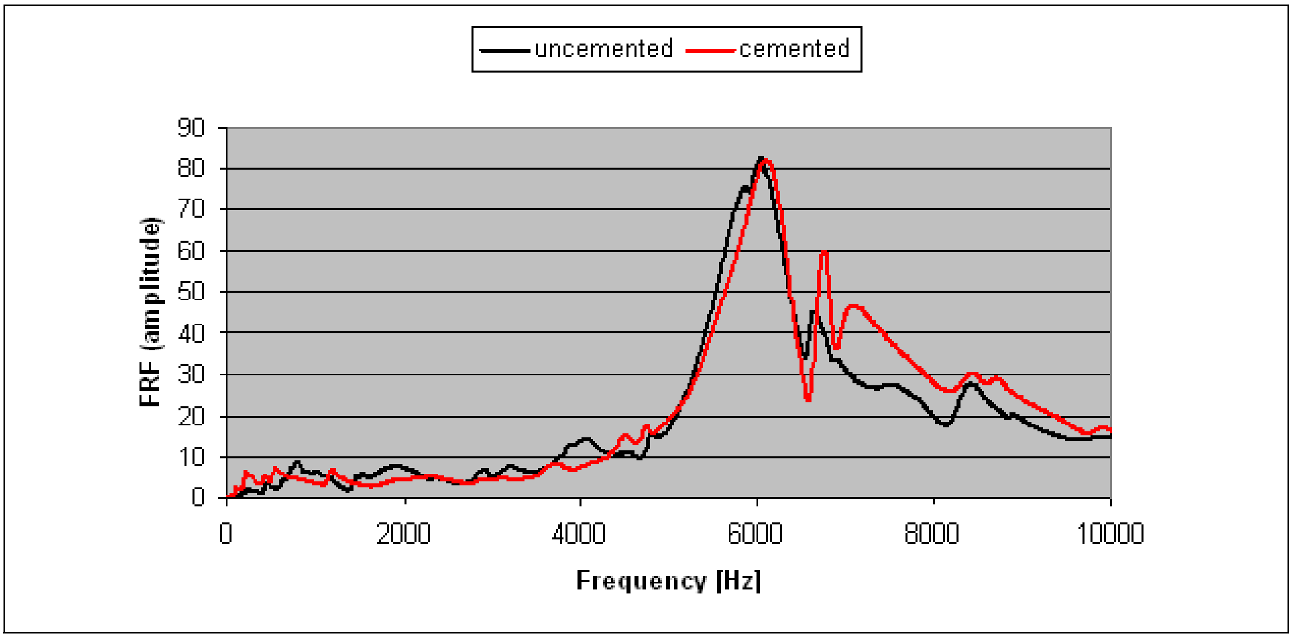

Figure 7: Partially cemented stem completely inserted in femur (example case 3)
FRF graphs for two stages: without cement (black) and cemented (red)

In order to analyse the FRF evolution for the case presented in fig. 7, the normalised cross correlation function was calculated (fig. 8).

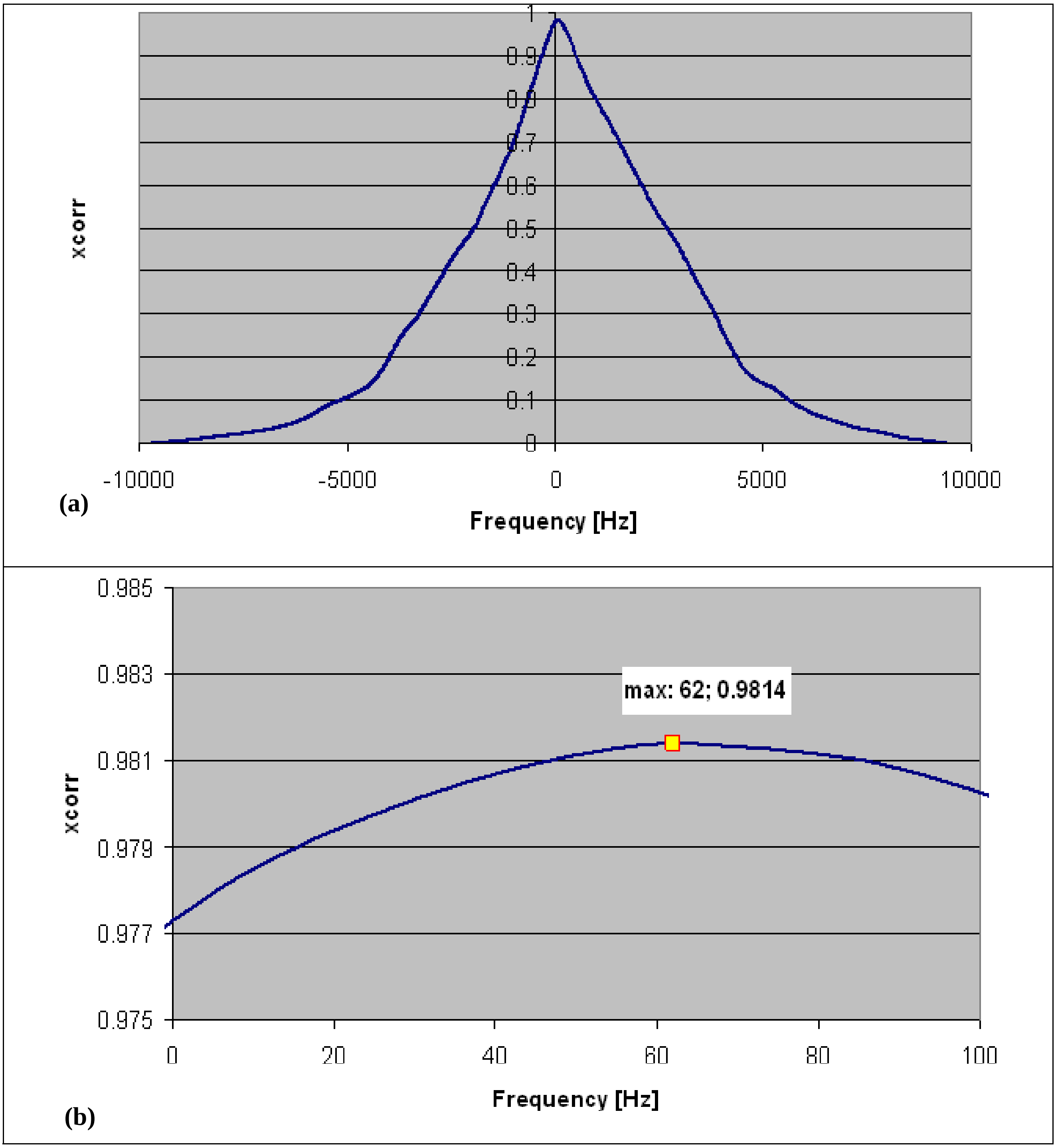

Figure 8: Normalised cross correlation function calculated for the FRF graphs represented in fig. 7 a: the whole graph; b: detail

In all cases the highest FRF peaks were found above 4000-5000 Hz.

3.2 Cementless stems

Eleven cases of cementless stems were studied and a typical example is presented in figure. 9. Figures 9a-c show the FRFs calculated for two successive insertion stages. Stage 0 corresponds to the FRF calculated after the stem was introduced in the femur by hand, stage 1 corresponds to the FRF calculated after the first hammer blow series, stage 2 after the second hammer blow series and so on. The surgeon needed 4 stages (0…3) to completely insert the stem in this case.

The evolution of Pearson’s correlation coefficient calculated for two successive FRFs is represented in fig. 9d. The normalised cross correlation function was also calculated for the same successive FRF pairs and presented in fig. 9e. The evolution of maximum values of cross correlation function can be observed in fig. 9f.

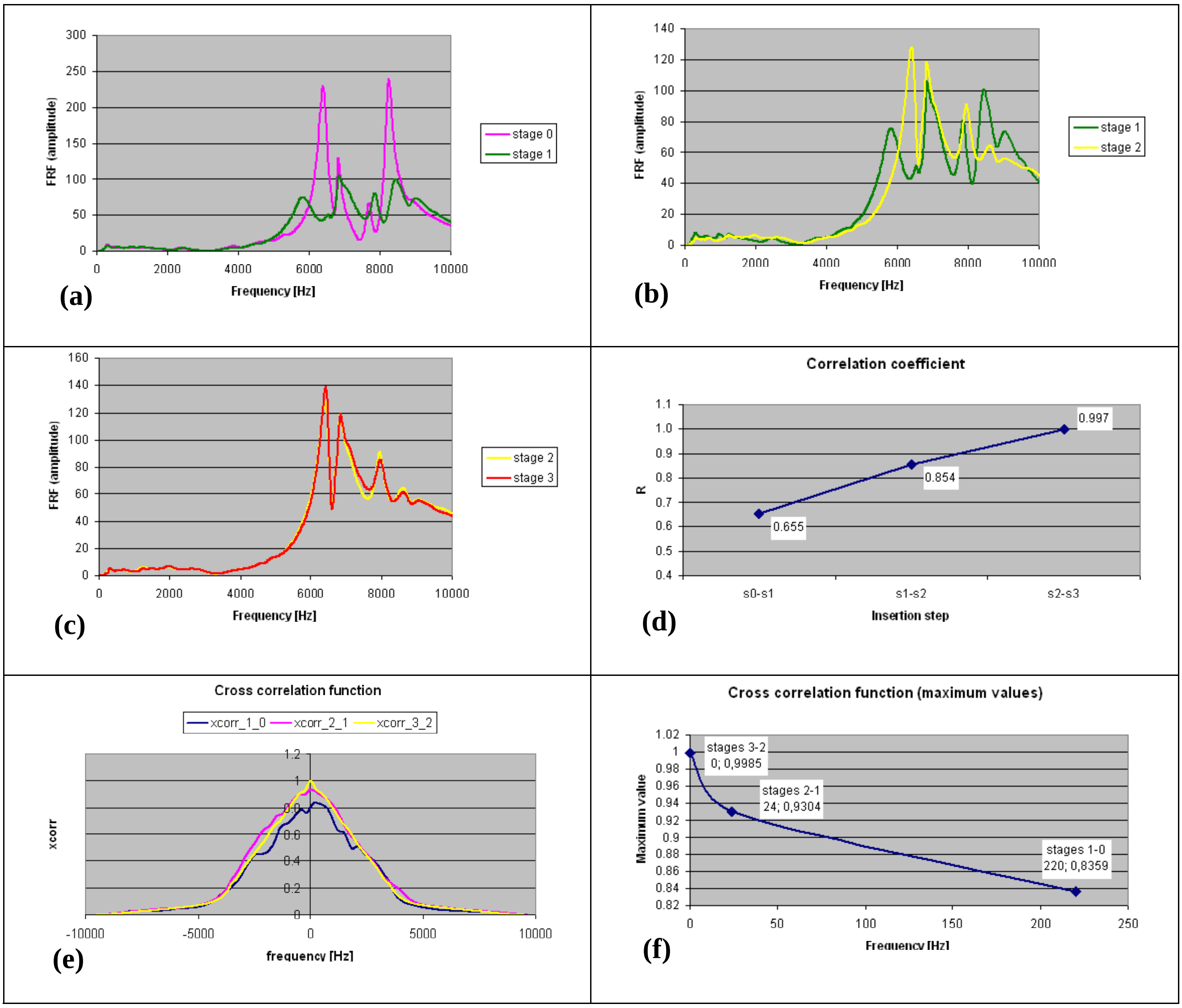

Figure 9: Cementless stem (example case 1)

a-c: FRF graphs for successive insertion steps;

d: Pearson’s correlation coefficients calculated for the FRF pairs represented in fig. 9 a-c

e: Normalised cross correlation functions calculated for the FRF pairs represented in fig. 9 a-c

f: Maximum values of the cross correlation functions represented in fig. 9 e

A similar example with five insertion stages is presented in figure 10.

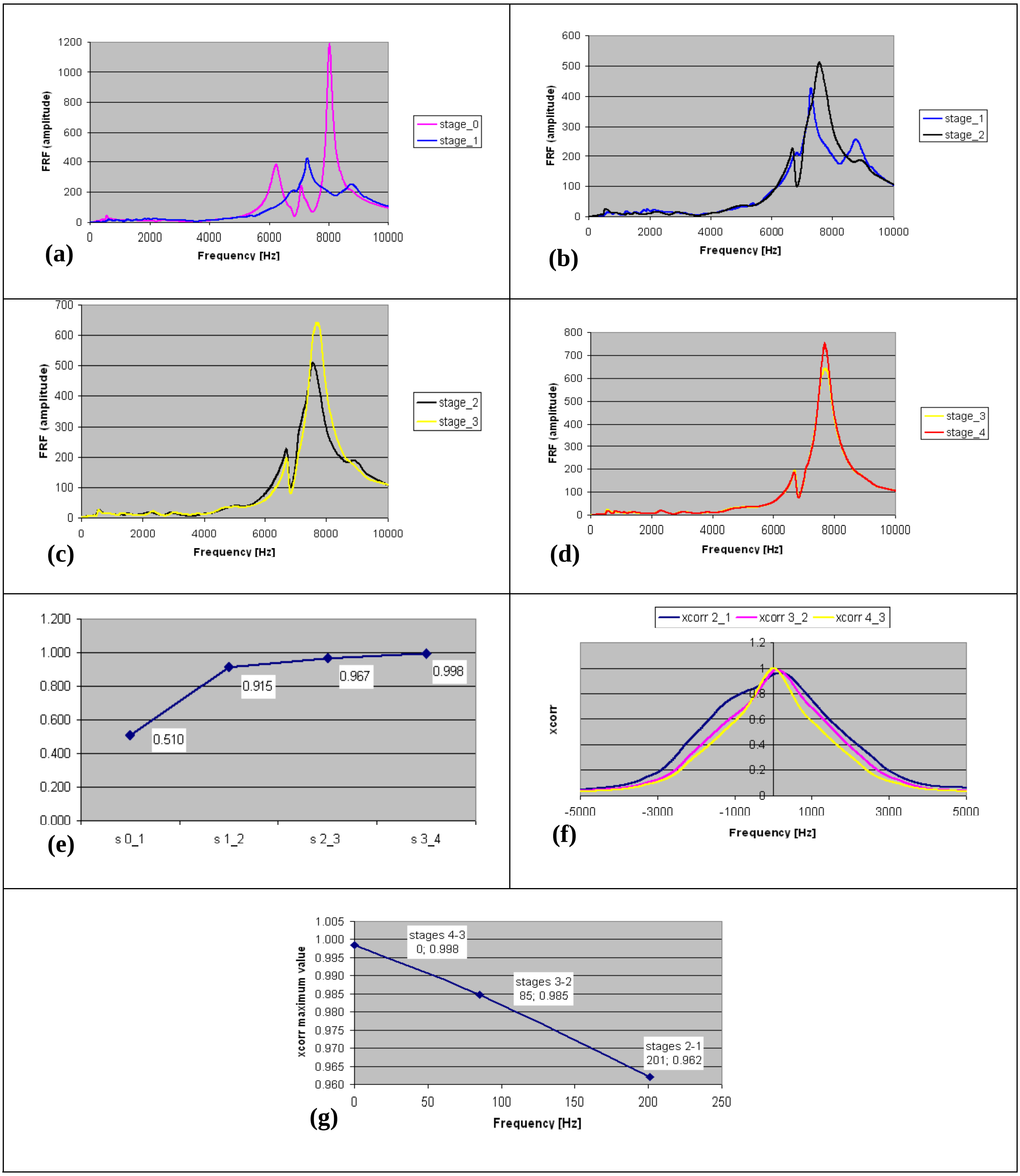

Figure 10: Cementless stem (example case 2)

a-d: FRF graphs for successive insertion steps;

e: Pearson's correlation coefficients calculated for the FRF pairs represented in fig. 10 a-d

f: Normalised cross correlation functions calculated for the FRF pairs represented in fig. 10 b-d

g: Maximum values of the cross correlation functions represented in fig. 10 f

The final Pearson’s correlation coefficients calculated for all the eleven cementless cases are shown in table 1.

Case No.	Pearson's coefficient
1	0.997
2	0.999
3	0.992
4	0.999
5	0.999
6	0.998
7	0.955
8	0.998
9	0.964
10	0.994
11	0.999
Average	**0.990**

Table 1: The Pearson’s correlation coefficients calculated between the FRFs corresponding to the final two insertion steps

4 Discussion

4.1 General

The structures analysed in this study are composed by stinger, hip stem and femur. Since during the insertion process the single variable element is the connection between the stem and the femur, a logical conclusion would be that the resonance frequencies of the studied structures are influenced only by this variable.

An FRF shift to the right indicates an increasing stiffness [23] of the stem-bone connection, thus an increasing stability of the implant. If the FRF does not change between two successive insertion stages, then the mechanical properties of the structure did not change by the additional hammer blows, thus the stem-bone connection is stable and the insertion end point is reached.

During the operation, the surgeon corroborated the information obtained by direct visual and tactile observation, with the information furnished by vibration analysis, to take the optimal decisions. The validity of the per-operative protocols should be assessed by an appropriate post-operative follow-up of the patients. In an ongoing clinical study, part of project OT/03/31, migration of the stems is followed up by Roentgen Stereophotogrammetric Analysis (RSA) and bone remodelling is followed up by Dual energy X-Ray Absorptiometry (DXA). Conventional follow-up by clinical examination, radiographs and standardised questionnaires is also part of the protocol.

The Pearson’s correlation coefficient was used to compare the similarity of two FRF graphs. Due to the fact that there is no linear dependence of one graph with respect to the other, the two graphs are identical if the correlation coefficient is 1.

The normalised cross correlation function between the current FRF graph and the previous FRF graph was used to assess the direction and the magnitude of the FRF graph shift. The abscissa of the maximum value of the cross correlation function indicates the displacement direction. A positive value means that the current FRF graph shifted to the right with respect to the previous FRF graph. The maximum value of the cross correlation function indicates the similarity of the two FRF graphs. When two graphs are identical, the cross correlation function becomes the autocorrelation function and its normalised maximum has the coordinates x=0 and y=1.

4.2 Partially cemented stems

For a partially cemented stem, the distal part is made thinner than the corresponding femoral cavity to allow the necessary space for the cement layer between the implant and the bone. The proximal part of the stem is designed to have direct contact with the bone and fills completely the corresponding cavity.

In the first stage, the stems are introduced in the femur without cement and, as a consequence, they are well fixed only in the proximal part. The stability of the same implants should increase in the second stage because the distal part is fixed in cement. In seven cases the FRFs indeed shifted to the right indicating an increased stiffness, i.e. an increased stability. An important change of the FRF graph shape was also observed, which indicates an important change of vibration modes.

In two cases the FRF change was not very important and the resonance frequencies corresponding to the highest FRF peaks did not substantially increase. The interpretation could be that the implant stability did not considerably change after cementation. Probably the stems were already quite well fixed in non cemented stage. An analysis using the cross correlation function (fig. 8) shows that the FRF graph shifted slightly to the right after cementation, thus the stability did improve somewhat.

The FRF graphs corresponding to the non cemented and cemented stages could be used in further studies as a reference for distal loosening and, respectively, well fixed hip stems.

4.3 Cementless stems

In a previous in vitro study [22,24] the criterion of Pearson’s correlation coefficient R=(0.99 +/- 0.01) between the FRFs of successive insertion stages was used as a quantitative threshold to stop the cementless stem insertion process. In per-operative conditions, the correlation coefficient between the last two FRFs was above 0.99 when the surgeon stopped the insertion, in nine of eleven cases (Table 1). In the other two cases, when the surgeon decided to stop the insertion because of suspected bone fragility, the final correlation coefficient reached lower values (0.955 and 0.964).

Although the FRF evolution is a good indication concerning the stability evolution, in some cases the FRF graph changes are complex and difficult to evaluate directly (fig. 9b). However, the cross correlation function graphs presented in fig. 9f and fig. 10g indicate a general displacement of the FRF to the right after each insertion stage, excepting the last one when the FRF graph did not change noticeably its shape nor position. The final FRF graphs are not an absolute indication of stability, but represent important information concerning the best stability that could be obtained in each case for its particular characteristics (stem geometry, bone quality etc.).

5 Conclusions and future work

The presented study shows that vibration analysis can be used to detect the insertion end point and to assess the implant stability in THR as a per-operative method.

During the insertion procedure, the change of boundary conditions and implant stability between different stages are reflected by the FRF evolution and the most sensitive frequency band is above 4 kHz.

Custom made hip stems are designed to fit and fill as much as possible the femoral cavity to obtain a good stability and their geometry is variable depending on the patient's femur characteristics. This variability complicates the comparison between the stabilities of different stems and the establishment of a general scale to evaluate the stability and the further evolution of custom hip implants. However, the follow-up of patients as part of an ongoing clinical study, and the analysis of a large number of FRF graphs could allow a classification depending on the stem geometry, femur properties and implant-bone contact characteristics.

Acknowledgements

This research was partially funded by a grant from the K.U.Leuven research council (OT/03/31).

Custom made hip prostheses provided by courtesy of Advanced Custom Made Implants S.A./N.V.

References

[1] R. M. Meek, D. S. Garbuz, B. A. Masri, N. V. Greidanus, C. P. Duncan, *Intraoperative fracture of the femur in revision total hip arthroplasty with a diaphyseal fitting stem,* J Bone Joint Surg [Am] 2004, 86A(3):480-5.

[2] Lippmann R K. *The use of auscultatory percussion for the examination of fractures*, J. Bone Jt Surg. 1932; 14, 118.

[3] Lowet G, Van Audekercke R, Van Der Perre G, Geusens P, Dequeker J, Lammens J. *The relation between resonant frequencies and torsional stiffness of long bones in vitro. Validation of a simple beam model.*, J. Biomechanics 1993; 26, pp. 689-696.

[4] Lowet G, Van Der Perre G. *Ultrasound velocity measurement in long bones: measurement method and simulation of ultrasound wave propagation 1996*; J. Biomechanics 29: 1255-1262.

[5] Nokes LDM. *The use of low-frequency vibration measurement in orthopaedics* 1999; Proc. Instn. Mech. Engrs. 213H: 271-290.

[6] Van Der Perre G, Lowet G. *In vivo assessment of bone mechanical properties by vibration and ultrasonic wave propagation.* Bone 1996; 18: 29S-35S.

[7] Roberts SG, Hutchinson TM, Arnaud SB, Kiratli BJ, Martin RB, Steele CR. *Noninvasive determination of bone mechanical properties using vibration response: A refined model and validation in vivo.* Journal of Biomechanics 1996; 29(1): 91-98.

[8] Van der Perre G. In: *Monitoring of Fracture Healing by Vibration Analysis and Other Mechanical Methods 1985*; (Eds. G. Van der Perre and A. Borgwardt-Christensen), *Proceedings of the Specialists Consensus Meeting, Leuven,* (Amersfoort, Leuven, Belgium).

[9] Nikiforidis G, Bezerianos A, Dimarogonas A, Sutherland C. *Monitoring of fracture healing by lateral and axial vibration analysis*. J. Biomechanics 1990; 23:323-330.

[10] Nakatsuchi Y, Tsuchikane A, Nomura A. *Assessment of fracture healing in the tibia using the impulse response method*. Journal of orthopaedic trauma 1996; 10 (1): 50-62.

[11] Meredith N, Shagaldi F, Alleyne D, Sennerby L, Cawley P. *The application of resonance frequency measurements to study the stability of titanium implants during healing in the rabbit tibia*. Clinical oral implant research 1997; 8: 234-243.

[12] Pattijn V, Van Lierde C, Van der Perre G, Naert I, Vander Sloten J. *The resonance frequencies and mode shapes of dental implants: Rigid body behaviour versus bending behaviour. A numerical approach*. Journal of Biomechanics 2006; 39 (5): 939-947.

[13] Huang HM, Chiu CL, Yeh CY, Lee SY. *Factors influencing the resonance frequency of dental implants*. Journal of Oral and Maxillofacial Surgery 2003; 61 (10): 1184-1188.

[14] Van der Perre G. *Dynamic analysis of human bones*. In: Functional Behaviour of Orthopedic Biomaterials 1984; Vol I: P. Ducheyne and G.W. Hastings, Eds., CRC Press, Boca Raton, 99-159.

[15] Rosenstein AD, McCoy GF, Bulstrode CJ, McLardy-Smith PD, Cunningham JL, Turner-Smith AR. *The differentiation of loose and secure femoral implants in total hip replacement using a vibrational technique: an anatomical and pilot clinical study*. Proc. Instn. Mech. Engrs. 1989; 203: 77-81.

[16] Collier RJ, Donarski RJ, Worley AJ, Lay A. *The use of externally applied mechanical vibrations to assess both fractures and hip prosthesis* In: *Micromovement in Orthopaedics*, A.R. Turner-Smith, Ed., University Press 1993, Oxford, 151-163.

[17] Li PLS, Jones NB, Gregg PJ. *Loosening of total hip arthroplasty; diagnosis by vibration analysis*. J Bone Joint Surg 1995; 77: 640-644.

[18] Li PLS, Jones NB, Gregg PJ. *Vibration analysis in the detection of total hip prosthetic loosening*. Med. Eng. Phys. 1996; 18: 596-600.

[19] Georgiou AP, Cunningham JL, *Accurate diagnosis of hip prosthesis loosening using a vibrational technique*. Clinical Biomechanics 2001; 16: 315-323.

[20] Jaecques S.V.N. Pastrav C. Vegehan E. Van der Perre G. *Analysis of the fixation quality of cementless hip prostheses using a vibrational technique*, *Proceedings of ISMA2004 International Conference on Noise and Vibration Engineering*, September 20 - 22, 2004, Eds. P. Sas and M. De Munck, K.U. Leuven, Belgium, ISBN 90-73802-82-2, pp. 443-456.

[21] Qi G, Mouchon WP, Tan TE, *How much can a vibrational diagnostic tool reveal in total hip arthroplasty loosening?* Clinical Biomechanics 2003; 18: 444-458.

[22] Pastrav L.C. Jaecques S.V.N. Deloge G. Mulier M. Van Der Perre G. *A system for intra-operative manufacturing and stability testing of hip prostheses*, *Proceedings of XIIIth international conference on New technologies and products in machines manufacturing and technologies (TEHNOMUS XIII)*, May 6-7, 2005, University “Stefan cel Mare”, Suceava, Romania, Published by University of Suceava, Ed. I. Dumitru, ISBN 973-666-154-7, pp. 505-510.

[23] W. Heylen, S. Lammens, P. Sas, *Modal Analysis Theory and Testing*, Katholieke Universiteit Leuven, Departement Werktuigkunde, Leuven (1997).

[24] Jaecques S. Pastrav L. Mulier M. Van der Perre G. *Determination of THR stem insertion endpoint by vibrational analysis*, in: R. Cabral, M. Cassiano Neves, C. Camilo, Eds., *Transactions of the EORS*, Vol. 15, 2005, p. 92, ISBN:90-9018444-9, published by Soc. Portuguesa de Ortopedia e Traumatologia.